

Analyses of eight internal fixation techniques of a fracture of the distal humerus by nonlinear FEM-Simulation, evaluating the generalized force deflection behavior in comparison to an intact bone

Werner Kolb¹, Ulrich Hindenlang²

1. Department of Trauma Surgery, Friedrich-Schiller-University Jena, Germany

2. LASSO Ingenieurgesellschaft, Leinfelden-Echterdingen, Germany

Abstract: A study of eight different internal fixation techniques of a fracture of the distal humerus is presented with four configurations of double or 3-plate osteosynthesis, using conventional 3.5-mm and locked 3.5-mm reconstruction plates. Dorsal (groups 1 and 3), 90° (groups 2 and 4), sagittal (groups 5 and 7) and 3-plate (groups 6 and 8) configurations were studied for elastomechanical properties of the constructs. A realistic bone representation was obtained by mapping the clinically measured CT-density distribution onto an inhomogeneous stiffness representation. Simplified loading situations of four generalized forces (tension and moments) were analyzed and the respective stiffnesses of the stabilized bone were compared to the stiffness of an intact bone. The applied modelization technique of the manual adaptation of plates to the outer surface of the bone, performed with the ANSA-morphing tool, is also presented.

Keywords: Biomedics, Elbow, Morphing, fracture of the distal humerus, internal fixation, conventional and locked 3.5-mm reconstruction plates, clinical CT, CT density distribution, natural stiffness of intact bone.

1. Introduction

Restoration of painless and satisfactory elbow function after a fracture of the distal humerus requires anatomic reconstruction of the articular surface, restitution of the overall geometry of the distal humerus, and stable fixation of fracture fragments to allow for early and full rehabilitation (O'Driscoll). In spite of the fact that surgical techniques for the treatment of fractures of the distal humerus have advanced substantially over the past 20 years, and are now quite sophisticated, the rate of complications remains high (Chapman). The anatomy of this area, combined with the presence of smooth cancellous bone, continue to present major problems to orthopaedic surgeons. The lateral column is approximately 20° valgus, relative to the midline of the humeral shaft,

whereas the medial column is at a 40° to 45° angle. From a lateral perspective, the capitellum is tilted 40° (Chapman) to 60° (Schatzker) anteriorly, and the trochlea is tilted 20°. The age-related osseous demineralization of the distal humerus, particularly in the capitellar region, is a major problem (Korner et al.). The weakest link of any internal fixation construct is the attachment to the bone (Holdsworth). Dunham et al. quantified the indentation strength and modulus of the distal humeral cancellous bone, finding that the posterior lateral region had lower modulus values. The regional variations in the indentation modulus suggest that the posterior lateral region should be avoided during fixation of implants or placement of screws. Stable fracture fixation still remains problematic, especially in elderly patients or in cases with metaphyseal comminution.

Five independent variables can be considered, in general, to evaluate the efficacy of an implant (Müller et al.):

- Bone quality and its evolution (remodeling).
- Geometry and position of the fractured fragments.
- The reduction of the fracture.
- The design of the implant employed.
- The location of the implant

The only variables, that can be chosen by the surgeon are the type of implant and its position (Cegonino et al.).

The ideal implant should provide adequate stability under physiological loads and the bone-implant interface should not be alternated under cyclic stress (Korner et al.). In a conventional plating technique, insertion and tightening of the plate screw generates an axial screw force, which compresses the plate onto the bone surface (Perren).



Figure 1. 3.5-mm reconstruction plate, 3.5-mm cortical screw (above), 4.0-mm cancellous screw (below)

In osteoporotic bone, commonly recommended fixation concepts fail because bone quality is poor (Gautier and Jacob). O'Driscoll and Jupiter et al. suggest parallel placement of the plates, or 3-plate fixation, to improve the fixation technique. The internal fixator is a new type of fixation, consisting of a plate and screws joined to the plate by means of threaded holes. This non-contact

plate has been introduced due to the importance of biological factors in internal fixation. By using an internal fixator with locked screw heads, the screw is loaded mainly in bending instead of pullout (Tepic and Perren). Recent developments allow for conventional compression, as well as locked internal fixation (locking compression plate, LCP, (Frigg).

Many authors have performed biomechanical studies of the distal humeral fractures. Most of these are based on clinical studies with conventional compression plates (Helfet and Hotchkiss). Korner et al. studied the biomechanical properties of two standard configurations of double plate osteosynthesis (dorsal or 90° configuration) with either conventional or locked 3.5-mm reconstruction plates. It was the first biomechanical test between conventional and locked 3.5-mm reconstruction plates for internal fixation of fractures of the distal humerus.

The advantage of computer simulations is that they allow for parametric analysis and personalized virtual tests; reducing the economic and social costs, compared to experimental techniques, and allowing for additional testing of different situations, impossible to simulate in real practice (Cegonino et al.).

We performed a finite element analysis of 8 different methods of internal fixation of distal humerus fractures according to the fixation techniques of Korner et al. (16), with 4 configurations of double or 3-plate osteosynthesis using conventional and locked 3.5-mm reconstruction plates. Our hypothesis was that the parallel or 3-plate fixation techniques, especially with the locked 3.5-mm reconstruction plate, are well suited for internal fixation of distal humeral fractures. The aim of our study was to compare the elastomechanical properties of the different constructs.

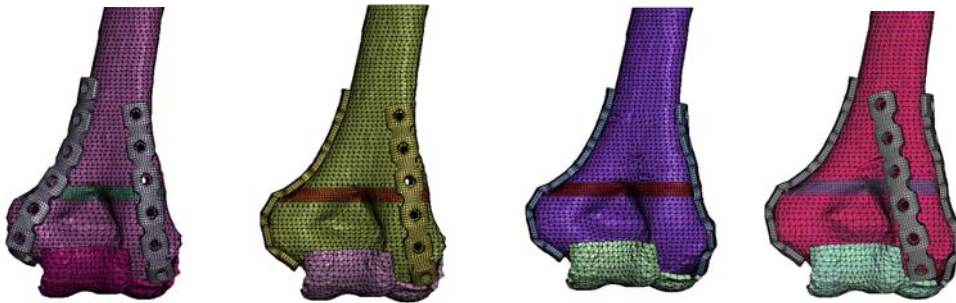


Figure 2. Dorsal plate position (groups 1-3), 90 degrees position (groups 2-4), parallel position (groups 5-7) and 3-plate fixation (groups 6-7) (from left to right)

2. Material and Methods

Abaqus[®] was used for finite element analysis and ANSA[®] (Beta CAE Systems, Thessaloniki, Greece) was applied for modeling. The humeral diaphysis defines the z-axis of the global system,

running distal to proximal. The x-axis lies in the frontal plane, through the axis of the humero-ulnar joint, and is at right angles to the z-axis. The y-axis points posterior.

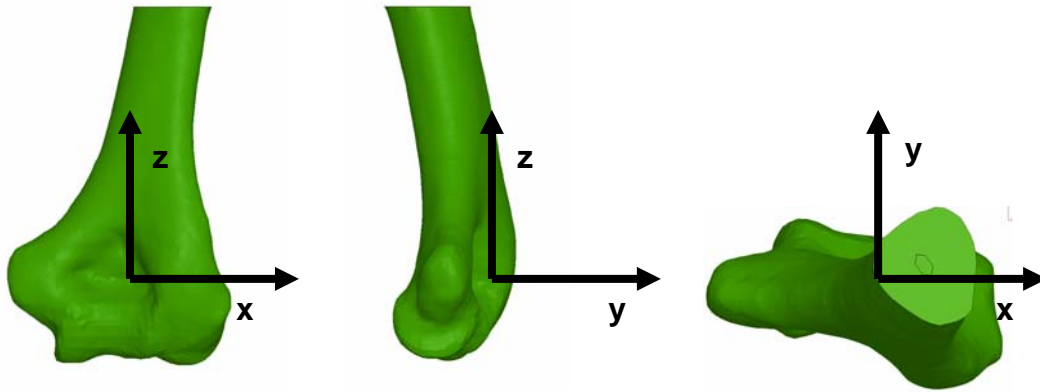


Figure 3. Definition of spatial position of the distal humerus.

The elbow of a 32 year-old man was scanned to obtain a set of slices by computed tomography. The distance between two slices was chosen to be 1 mm in the epiphysis and the trochlea, and 5 mm in the diaphysis. The geometry, and associated mesh, was reconstructed from these slices.

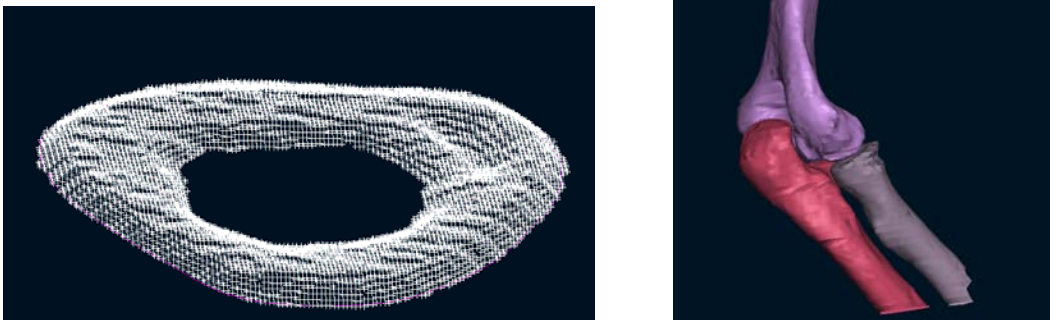


Figure 4. Density distribution (CT-section) and reconstructed elbow

A surface grid, made up of triangular elements was created. This was the basis for a pentahedron and tetrahedron volume model with 67785 elements and 20916 nodes. The distal part of the humerus was considered an inhomogeneous isotropic linear elastic material. The distribution of density within the humerus, which is correlated to the Hounsfield values of the CT, was used to map the inhomogeneous stiffness to all volume elements at their exact position in space. The

proportionality between the Hounsfield units HE and Young's Modulus for two regions, as defined by Rho et al., was used, (Hounsfield values ranged from 1 to 256):

$$HE = (\mu_{material} - \mu_{H2O}) / \mu_{H2O} \text{ so the maximum density is } 256 HE = 1.9976 \text{ g/cm}^3$$

$$E \leq 13.8 \text{ GPa: } E = 5546 \rho^{1.33}$$

$$E > 13.8 \text{ GPa: } E = 87 \rho^{7.40}$$

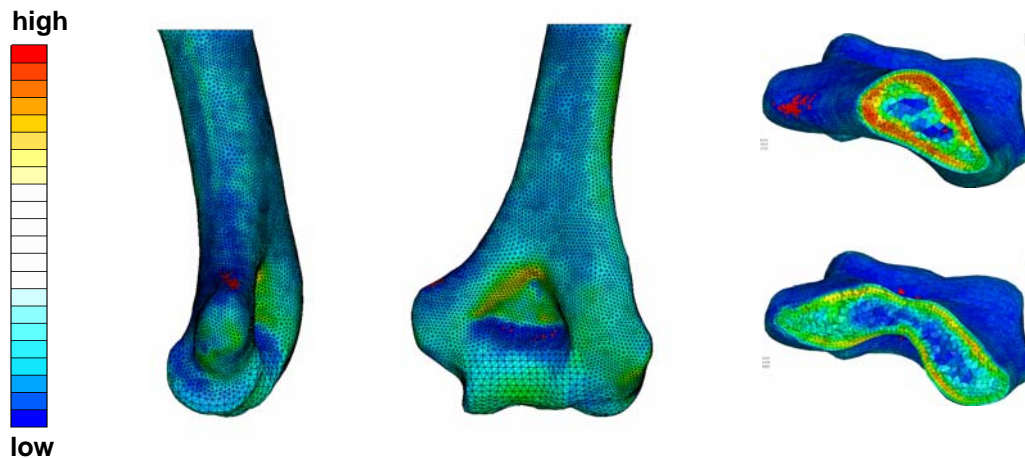


Figure 5. Distribution of density ~ stiffness

The range of Young's moduli was from 25 to 19800 MPa. The Poisson's ratio was chosen to be 0.3. This is a very simplified model, because bone is heterogeneous, non-linear, and anisotropic (Dunham et al.). A fracture model with a 5-mm supracondylar osteotomy gap, simulating metaphyseal comminution (AO type 13-A3.3) with a Young's modulus of 10 Mpa, was performed.

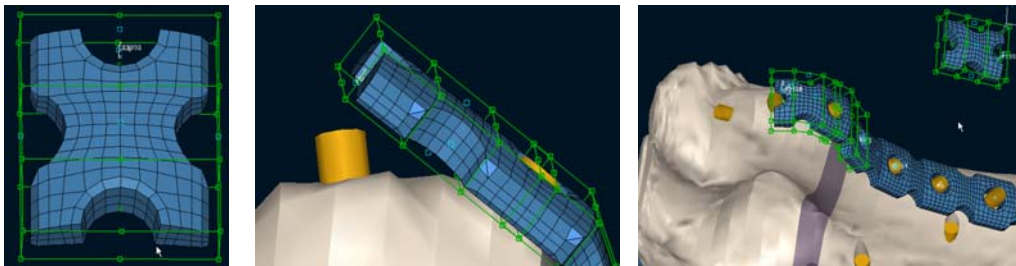


Figure 6. Adaptation of the 3.5-mm reconstruction plate onto the surface of bone

The geometry of the plates was measured by hand, since it was not supplied by the manufacturer.

With the morphing tool of ANSA, a representative specimen was bent artificially onto the surface of the distal bone (Fig. 6). The 3.5-mm reconstruction plates were modeled to the surface of the humerus according to the different configurations (Fig. 2). The isotropic elastic material properties of the 3.5-mm reconstruction plates (titan alloy) were assumed to be constant (Young's modulus 110 GPa), the Poisson's ratio of 0.3 eliminates any influence of hardening effects. All materials were defined only for elastic behavior, because the main topic of this investigation was the comparison of the stiffness sensitivity due to fixed angled and conventional compression screws

The screws were modeled with beam elements, representing the correct stiffness of the shaft; the screw head and thread were simply represented by stars, idealized by small beams. The fixed angled and conventional fixed situation at the screw head was modeled by joining the head star beams to the shaft by a multi-point-constrained definition, joining the rotational degrees of freedom for the fixed configuration. A pretension was introduced in the shaft, representing the tightening torque. The threads of the shaft were fixed at cylindrical holes drilled in the distal humerus, corresponding to the distance of the standard screws.

A standard contact definition between the plates and outer surface of the corticalis was used with a small coefficient of friction (0.01).

To apply near-physiological loading conditions, the loads were chosen based on the studies of An et al.: for anterior and posterior bending, and for torsion and axial compression. These generalized forces were applied by defining a center point in the middle third of the shaft of the humerus. Loads were applied at an angle of 15° through the axis of the humero-ulnar joint. To minimize complications due to the embedding of the humerus, the distal humerus was fixed through the cartilage in three planes. The cartilage of the distal humerus was modeled with a Young's modulus of 5 MPa, making force transfer as realistic as possible.

For loading cases:

- N_z , normal force acting in z-direction (250 N)
- M_x , bending moment about x-axis (4,5 Nm)
- M_y , bending moment about y-axis (4,5 Nm)
- M_T , torsional moment about z-axis (1,6 Nm)

Geometrical nonlinear static solutions were performed for 4 different internal fixation configurations, with conventional and locked 3.5-mm reconstruction plates, as well as the intact distal humerus without trauma (see figure 2).

1. intact distal humerus (called *intact*)
2. dorsal configuration (called *dorsal*)
3. parallel configuration (called *lateral*)
4. 90° configuration (called *90-grad*)
5. 3-plate configuration. (called *3-Platten*)

3. Results

The aim of the present investigation was to consider the different load-deflection behavior of the above configurations, and the following results were extracted:

- total deflection leading to representative stiffness
- maximum principal stress in the distal humerus
- maximum von-Mises stress in the 3.5-mm reconstruction plates.

A comparison of these results is given below in figures, the blue bars represent the locked 3.5-mm reconstruction plates and the red ones the conventional 3.5-mm reconstruction plate (Figs. 7-14).

In comparison to the intact bone, all reconstructed fractures had lower stiffness. The strongest configuration was represented by the 3-plate-configuration, and the weakest was the dorsal configuration. The stiffness of both the 90°- and lateral configurations were found in between. Only the stiffness of the locked 3-plate configuration reached under frontal bending the stiffness of the intact humerus. The fixed angled situation created a stiffer reaction for all investigated situations, as previously hypothesized.

Generally, the fixed angle screw-versions show higher stress in the implants. The conventional fixation techniques show higher stress level at the surface of the bone, except for the 90° configuration under compression and frontal bending. Since the loading is identical for all configurations, the highest stress in the implants is found near the fracture zone (except for the 3-plate configuration). The highest von-Mises stress was detected in the locked 90° configuration under frontal bending, followed by the conventional dorsal and lateral configurations. The difference between the fixed angle and conventional compression screw configurations was quite small, except for the dorsal configuration.

The most important principal stresses within the humerus under frontal bending were found in the 90-Grad configuration, followed by the dorsal, lateral, and the 3-plate-configurations.

The following figures compare the stiffness with respect to the intact humerus, as well as the maximum stress found in the humerus and implant.

A series of four plots show the load paths within the intact bone for the different load cases under consideration. The strongest (3-plate-) and weakest (dorsal) configurations von-Mises stress, for the fixed angle and conventional compression screws, are depicted for a direct comparison.

3.1 Compression

3.1.1 Stiffness

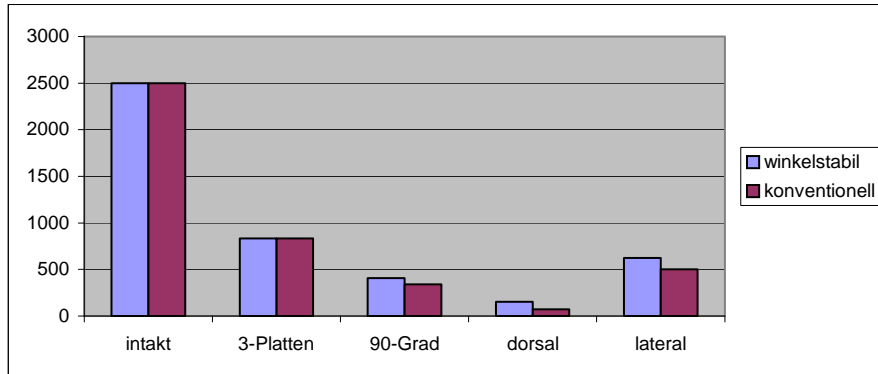
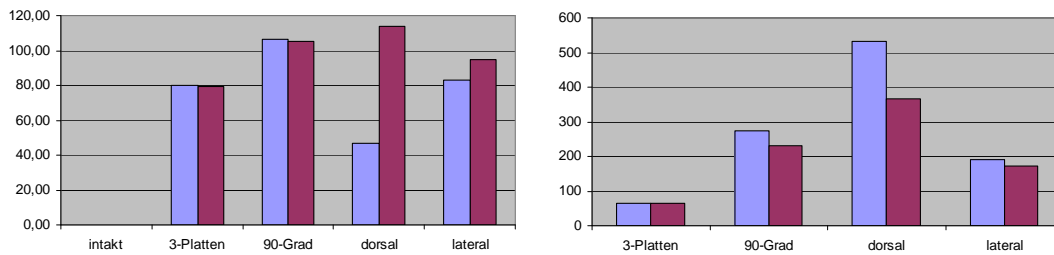


Figure 7. Stiffness under compression

3.1.2 Stress



Principal stress (N/mm²) in the bone

Maximal von-Mises stress in the plates

Figure 8-A and 8-B Stress (N/mm²) under compression

3.2 Sagittal bending

3.2.1 Stiffness

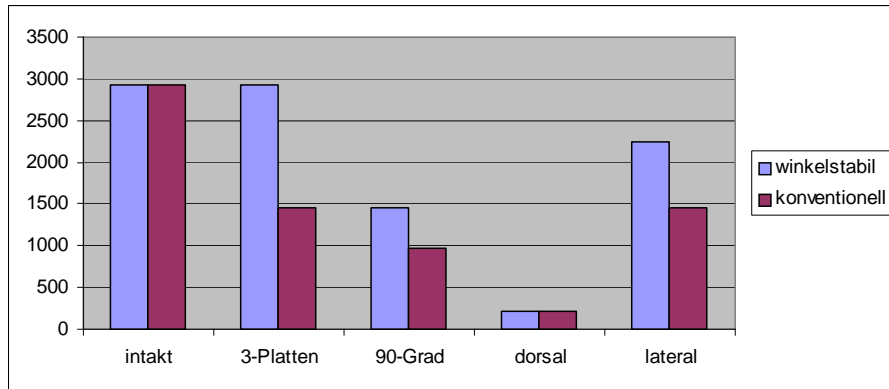
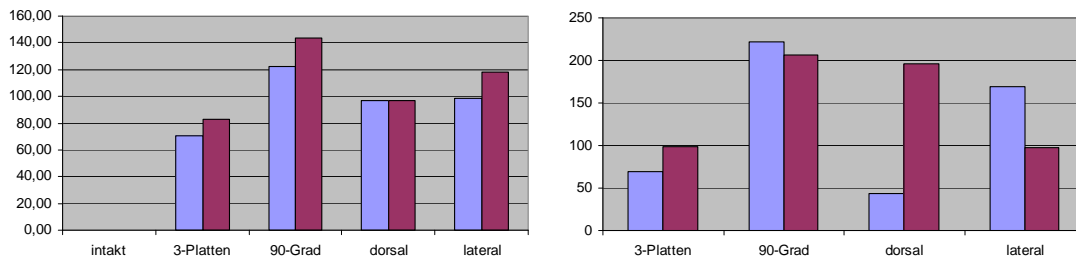


Figure 9. Stiffness under sagittal bending M_y

3.2.2 Stress



Principal stress (N/mm^2) in the bone

Maximal von-Mises stress in the plates

Figure 10-A and 10-B Stress (N/mm^2) under sagittal bending M_y

3.3 Frontal bending

3.3.1 Stiffness

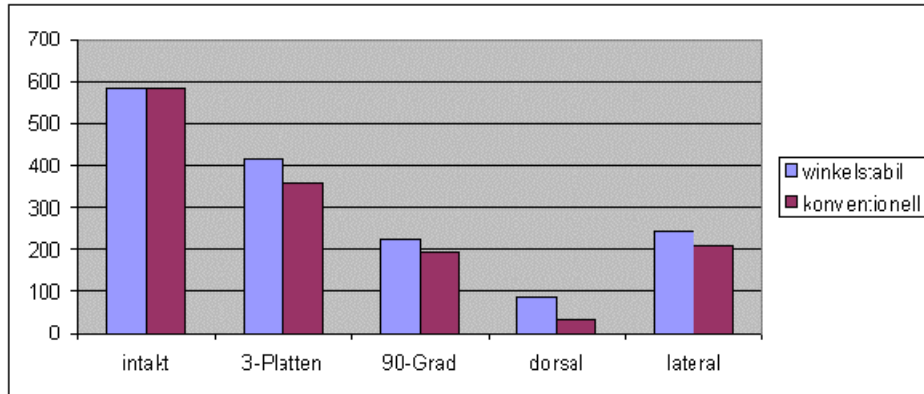


Figure 11. Stiffness under frontal bending M_x

3.3.2 Stress

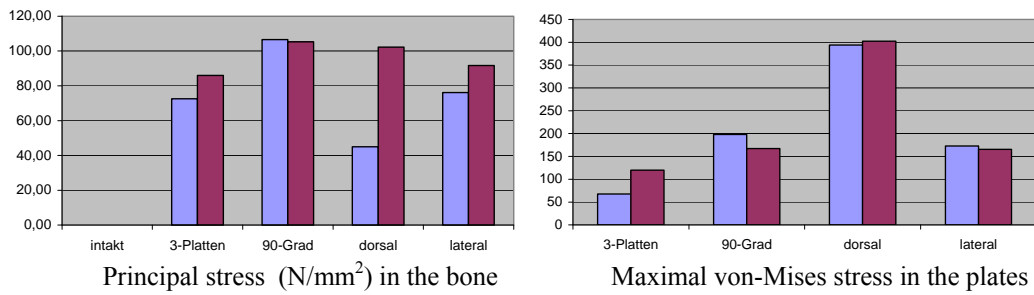


Figure 12-A and 12-B Stress (N/mm²) under frontal bending M_x

3.4 TORSION

3.4.1 Stiffness

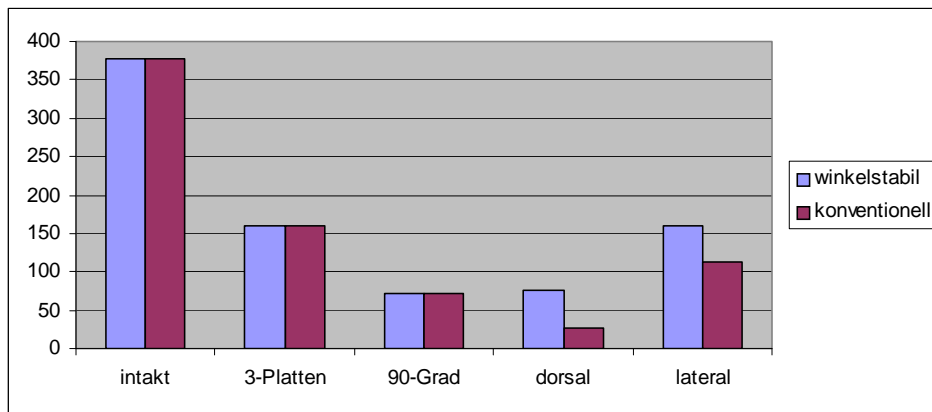
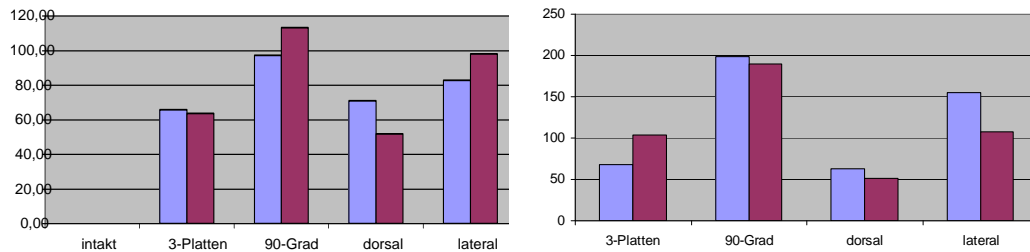


Figure 13. Stiffness under torsion M_T

3.4.2 Stress



Principal stress (N/mm^2) in the bone

Maximal von-Mises stress in the plates

Figure 14-A and 14-B Stress (N/mm^2) under torsion M_T

3.4.3 Plots

Intact bone under loading

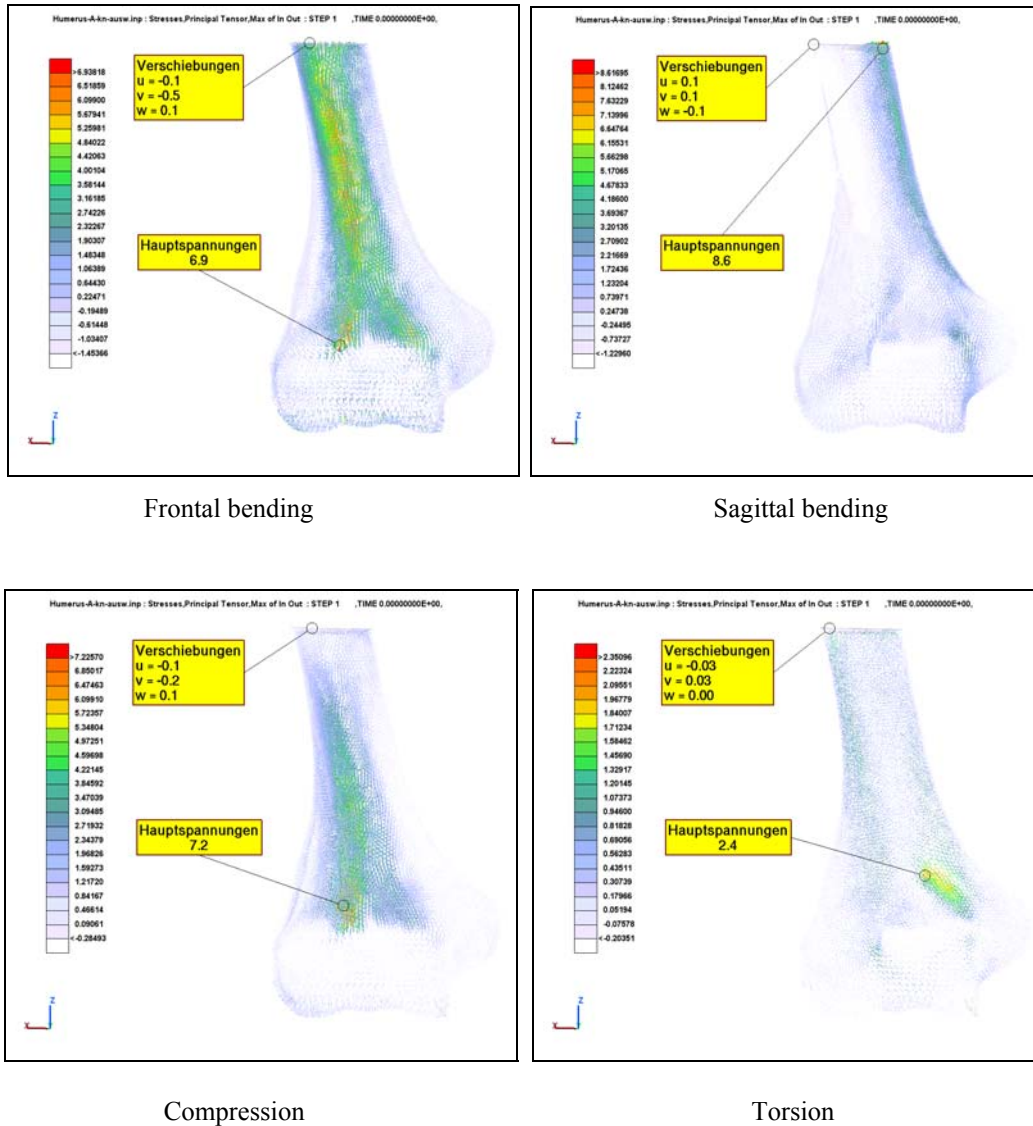


Figure 15. Principal stress in the intact humerus under different loading situations

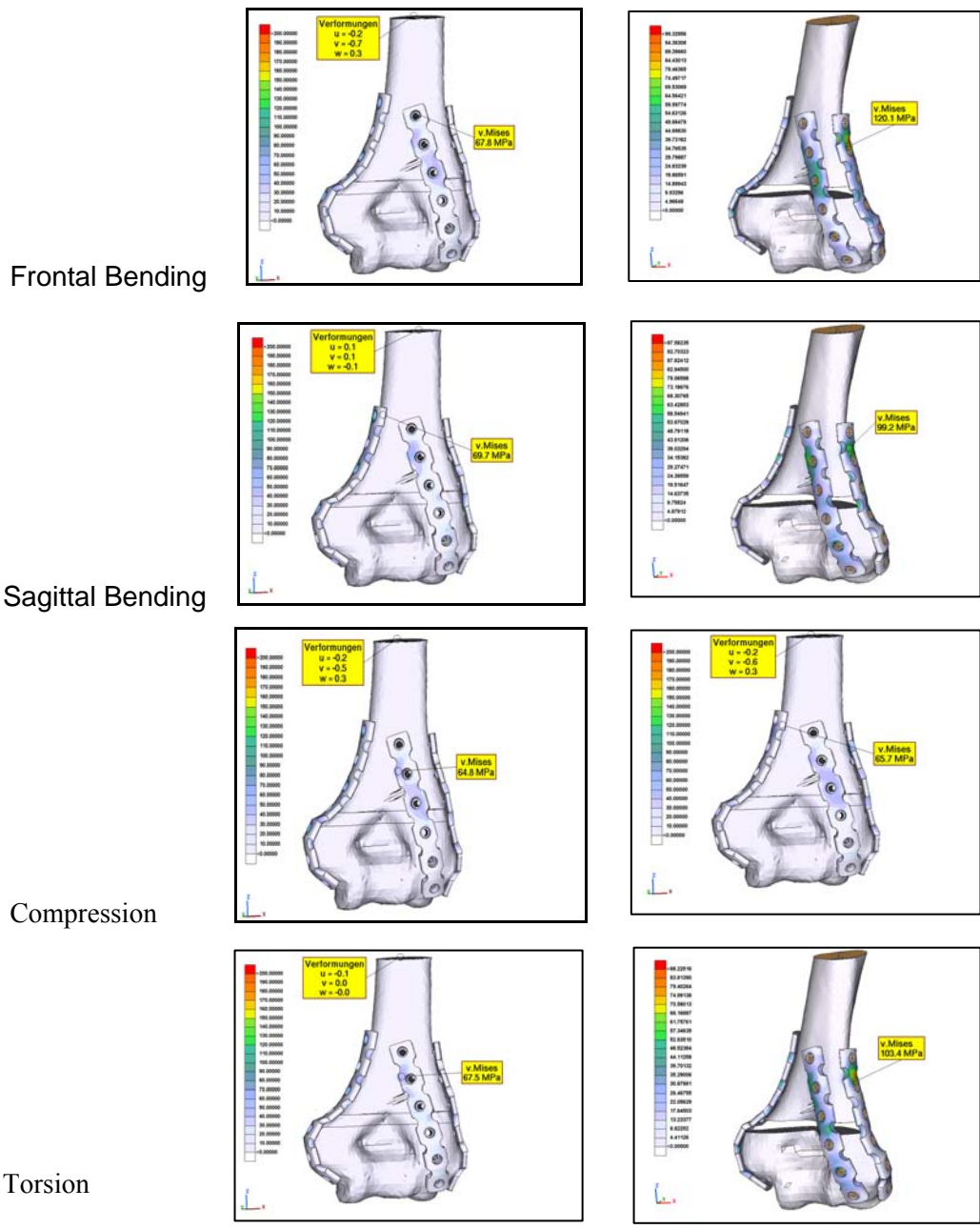


Figure 16. Von Mises stress in the 3-plate configuration under different loading situations, left fixed angle, right conventional compression screws

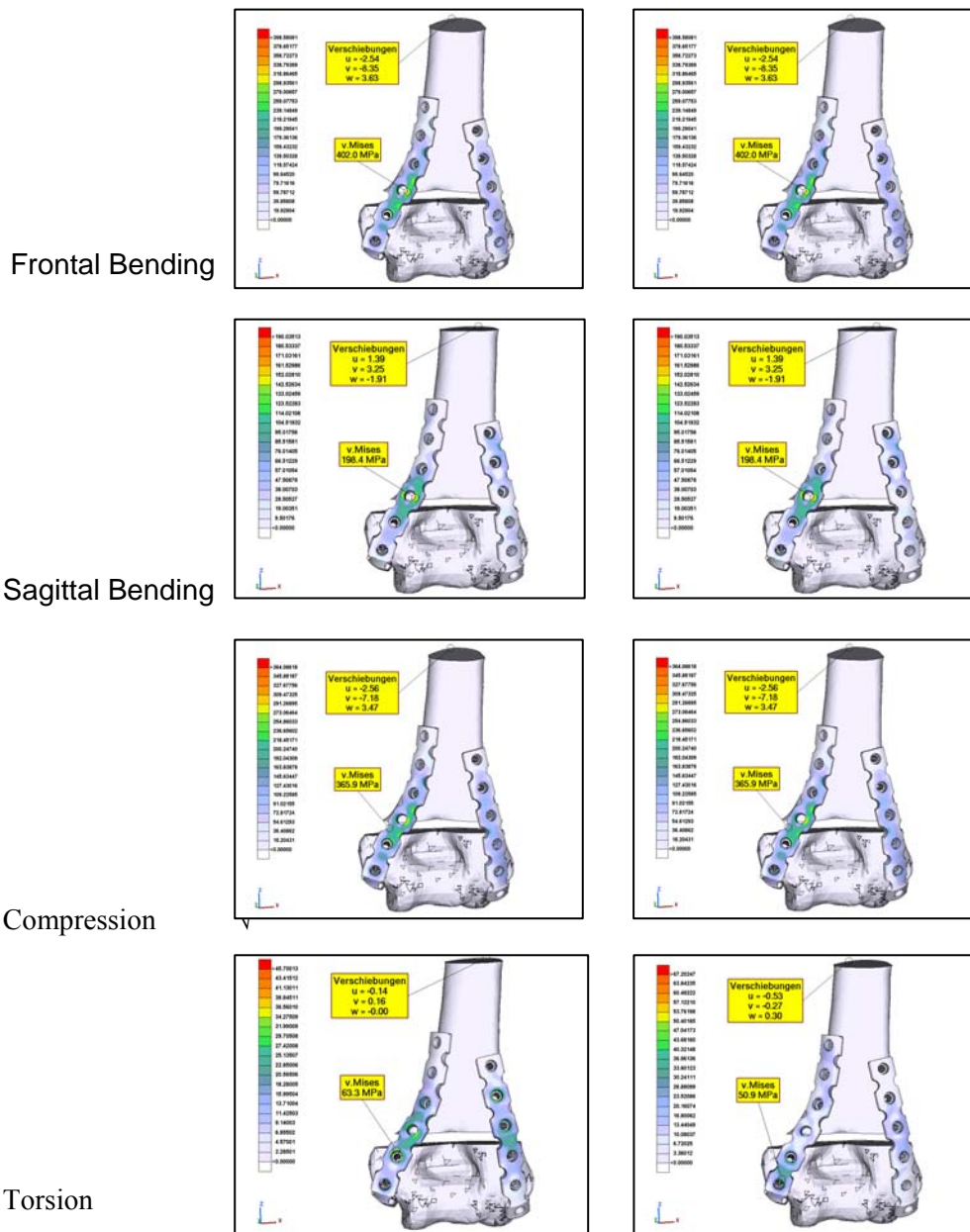


Figure 17. Von Mises stress in the dorsal configuration under different loading situations, left fixed angle, right conventional compression screws

4. Discussion

The aim of open reduction and internal fixation of fractures of the distal humerus is the restoration of the anatomy and stable fragment fixation to sustain posttraumatic stiffness of the elbow. The number of osteoporotic multifragmentary fractures increases with the aging population (13-C2 or 13-C3 according the AO-Classification (Müller ME et al.), with fractures at both the supracondylar and intercondylar regions. The double plate osteosynthesis in the dorsal or 90° configurations are the preferred methods of internal fixation. In biomechanical tests, the 90° configuration was the most stable fixation (Helfet and Hotchkiss). We observed the same effect in our simulations, comparing only the dorsal and 90° configurations. These two usual fixation techniques were modified by Jupiter et al. and O'Driscoll, because these tests did not consider the increasing number of osteoporotic multifragmentary intraarticular fractures. Fixation of more than one or two short monocortical screws in the distal fragment is often impossible.

In vivo, the load on the posterolateral bone implant interface increases, resulting in failure of fixation in the lateral column (O'Driscoll). O'Driscoll suggests the parallel placement in the sagittal plane, linking the plates together through the bone, thereby creating the architectural equivalent of an arch, and offering the greatest biomechanical stability for comminuted fractures of the distal humerus. Jupiter and Ring popularized the 3-plate osteosynthesis for comminuted distal humerus fractures. These authors did not think that double plate osteosynthesis, with posterolateral fixation, is strong enough to achieve stability of the humeral columns, and to obtain satisfactory results in these difficult fractures. Our study, considering the natural stiffnesses of the different configurations, strongly supports these experiences.

The disadvantage of our investigation is the use of non-osteoporotic bone of a young man, however the advantage is the objective comparison of well-defined loading and boundary conditions, allowing precise sensitivity analysis on basis of a clinical measured humerus.

5. Conclusion

This study determined the von Mises stresses in the implant, and main stresses in the humerus at different configurations of the double or 3-plate fixations of extraarticular distal humerus fractures in finite element analysis. The maximum stresses in bending and compression were found in the implant of the radial column. For the dorsal configuration, the elastic limit for compression is already reached. As the material model is simplified, and no inelastic relaxation at high local stresses is realized, a failure prediction is not performed and would not be meaningful. The virtual comparison of the different fixation techniques indicates no important difference of the investigated screw fixation in the plates. The configuration of the plates is the significant difference stated in this study. In vivo, there is a lower indentation modulus in the posterior lateral region of the distal humerus. The load on the posterolateral bone implant interface increases, resulting in failure of fixation in the lateral column in comminuted distal humerus fractures. Therefore, we suggest the parallel placement of two plates in the sagittal plane; or, if possible, the 3-plate fixation for comminuted distal humerus fractures.

6. References

1. Amis A.A. et al. 1979. The derivation of elbow joint forces, and their relation to prosthesis design. *J Med Eng Technol.* Sep;3(5):229-34.
2. An K.N., et al. 1989. Physiological considerations of muscle force through the elbow joint. *J Biomech.* 22(11-12), 1249-1256.
3. An K.N., Morrey B.F., 2000. Biomechanics of the elbow, in Morrey, B.F., (Ed.), *The elbow and its disorders* third ed., WB Saunders, 43-60.
4. Cegonino J. et al., 2004. A comparative analysis of different treatments for distal femur fractures using the finite element method. *Comput Methods Biomech Biomed Engin.* 7, 245-56
5. Chapman M.W., 2001. Fractures and dislocations of the elbow and forearm, in Chapman M.W., (Ed.), *Chapman's Orthopaedic Surgery*, Lippincott Williams & Wilkins, Philadelphia, 481-529.
6. Dunham C.E., et al. 2005. Mechanical properties of cancellous bone of the distal humerus. *Clin Biomech* 20, 834-838.
7. Frigg R., 2001. Locking Compression Plate (LCP): An osteosynthesis plate based on the dynamic compression plate and the Point Contact Fixator (PC-Fix). *Injury* 32, SB63-SB6.
8. Gautier E., Jacob R.P., 2004. Biomechanics of Osteosynthesis by Screwed Plates, in Poitout D.G., (Ed.), *Biomechanics and Biomaterials in Orthopedics*. Springer, London, 330-350.
9. Helfet D.L., Hotchkiss R.N., 1990. Internal fixation of the distal humerus: a biomechanical comparison of methods. *J Orthop Trauma* 4, 260-264.
10. Helfet D.L., et al., 2003. Open reduction and internal fixation of delayed unions and nonunions of fractures of the distal part of the humerus. *J Bone Joint Surg Am.* 85-A, 33-40.
11. Henley M.B., et al., 1987. Operative Treatment of intraarticular fractures of the distal humerus. *J Orthop Trauma* 4, 260-264.
12. Holdsworth B.J., 2000. Humerus: distal, in Ruedi T.P., Murphy W.M. (Eds.), *AO Principles of Fracture Management*, Thieme, Stuttgart New York: 307-321.
13. Husikes R., Stolk J., 2005. Biomechanics and preclinical testing of artificial joints: The hip, in: Mow V.C., Huiskes R. (Eds.), *Basic Orthopaedic Biomechanics and Mechano-Biology*, Lippincott Williams & Wilkins, 585-656.
14. Jupiter J.B., et al., 1985. Intercondylar fractures of the distal humerus. An operative approach. *J Bone Joint Surg Am* 67, 226-239.
15. Korner J., et al., 2003. The LCP-concept in the operative treatment of distal humerus fractures – biological, biomechanical and surgical aspects. *Injury* 34 [suppl 2], S-B20-S-B30.
16. Korner J., et al. 2004, A biomechanical evaluation of methods of distal humerus fracture fixation using locking compression plates versus conventional reconstruction plates. *J Orthop Trauma*, 18, 286-293.
17. Letsch R., et al., 1989. Intraarticular fractures of the distal humerus. Surgical treatment and results. *Clin Orthop* 241, 238-244.

18. Müller M.E., et al., 1990. The comprehensive Classification of fractures of the Long Bones. Springer, Berlin Heidelberg New York.
19. Müller M.E., et al. 1991. Manual of Internal Fixation, Springer, Berlin, 485-500.
20. O'Driscoll S.W., 2005. Optimizing stability in distal humeral fractures. J Shoulder Elbow Surg 14, 186S-164S.
21. Perren S.M., 2002. Evolution of the internal fixation of long bone fractures. J Bone Joint Surg B 84, 1093-1110.
22. Ring D., Jupiter J.B. 2000. Fractures of the distal humerus. Orthop Clin North Am 31, 103-113.
23. Rho J.Y. et al, 1995. Relations of mechanical properties to density and CT numbers in human bone. Medical Engineering and Physics.17:347-355
24. Schatzker J., 2005. Fractures of the Distal End of the Humerus (13-A, B and C), in Schatzker J., Tile M., (Eds.), The Rationale of Operative Fracture Care. Springer, Berlin Heidelberg New York, 103-121.
25. Tepic S., Perren S.M., 1995. The biomechanics of the PC-Fix internal fixator. Injury 26, 2SB5-SB10.